16th World Conference on Earthquake, 16WCEE 2017

Santiago Chile, January 9th to 13th 2017

Paper N° 235

Registration Code: S-Y1459408815

A SPECTRAL ACCELERATION BASED INTENSITY MEASURE FOR P-DELTA VULNERABLE FRAMES IN THE COLLAPSE LIMIT STATE

C. Adam(1), D. Kampenhuber(2), L.F. Ibarra(3)

(1) Professor, Unit of Applied Mechanics, University of Innsbruck, christoph.adam@uibk.ac.at
(2) Postdoc, Unit of Applied Mechanics, University of Innsbruck, david.kampenhuber@uibk.ac.at
(3) Assistant Professor, Department of Civil and Environmental Engineering, University of Utah, luis.ibarra@utah.edu

Abstract

The efficiency of a recently introduced spectral based intensity measure (IM) is assessed, used for the assessment of the seismic collapse capacity of highly inelastic frame structures with deteriorating backbone curve vulnerable to the degrading effect of gravity loads (P-delta effect). This IM is derived from the geometric mean of the spectral pseudo-acceleration over a certain period interval considering period elongation due to inelastic deformations and gravity loads, as well as higher mode effects. The IM optimization is achieved by using the mode in which 95% of the effective modal mass is exceeded as a lower bound period of the averaging interval. The IM upper bound period is 1.6 times the fundamental period. The 5%-damped spectral pseudo-acceleration at the system's fundamental period is the benchmark IM. In a parametric study on generic frames, characteristic structural parameters are varied to quantify their impact on the performance of the IMs. The proposed IM minimizes collapse capacity due dispersion due to record-to-record variability for one-story and multi-story structures. Compared to the benchmark IM, the "optimal" IM increases the efficiency in average by about 20% for material non-deteriorating structures, and by 30% for medium material deteriorating systems.

Keywords: collapse capacity; efficiency; geometric mean of spectral acceleration; intensity measure; P-delta effect

1. Introduction

In earthquake engineering analysis an intensity measure (IM) is used to quantify the severity of a seismic event and the ground motion uncertainty, represented by one parameter or a vector of a few parameters related to a set of appropriately selected earthquake records. The IM also serves as a scale factor for non-linear dynamic analysis. Since there is no unique definition of intensity of an earthquake record, several IMs have been proposed. They can be classified into (a) elastic ground motion based scalar IMs such as peak ground acceleration (PGA), peak ground velocity (PGV) and peak ground displacement (PGD), (b) elastic and inelastic spectral based IMs such as spectral acceleration and spectral displacement at the fundamental period of the structure, as well as spectral values related to higher modes effect or period elongation (see e.g., [1 - 9]), and (c) vector valued IMs (e.g., [6, 10]). Currently, the most widely accepted IM is the 5% damped pseudo-spectral acceleration at the (fundamental) period of the structure, T_1, which serves in the present study as the benchmark IM.

Although many advanced IMs have been proposed, there are still some limitations such as the derivation of attenuation relations, the selection of the spectral values in case of higher modes and period elongation incorporation, and their validation for several structural systems, among others. In addition, most studies on the suitability of commonly used IMs (e.g., Jalayer et al. [11], O'Donnell et al. [12]) do not focus on the collapse limit state.

According to Luco and Cornell [3] and Bianchini et al. [4], an appropriate IM should comply with four properties. The first property is the *hazard computability* (*practicability*), i.e., for the IM appropriate ground motion prediction equations must be available to quantify the ground motion hazard at the site. The property of *efficiency* refers to the record-to-record (RTR) variability of peak structural response. It is measured by an appropriate Engineering Demand Parameter (EDP), and should be low at any level of the IM. The more efficient an IM is, the smaller is the number of ground motion records required to predict the structural response within a certain confidence level. The property of *sufficiency* describes the conditionally statistical independence on an IM on seismological characteristics, such as the magnitude, M_W, and the source-to-site distance, R. The fourth property is *scaling robustness*, which refers to the independence of the IM from scaling factors.

More recently, IMs based on the geometric mean of spectral pseudo-acceleration over a specific period interval have attracted the attention of several researchers. The studies of Tsantaki [13], Kampenhuber [14] and Tsantaki et al. [15] have shown that for P-delta vulnerable single-degree-of-freedom (SDOF) systems an IM based on the geometric mean concept of spectral accelerations satisfies better the properties of efficiency and sufficiency, compared with outcomes of benchmark studies [16, 17], where the 5% damped spectral pseudo-acceleration at the structural period has been used as IM. Adam et al. [8] analyzed the efficiency of this IM for collapse prediction of three sets of P-delta vulnerable frame structures. Recently, Eads et al. [9] evaluated the efficiency and sufficiency of a similar IM for collapse prediction using almost 700 moment-resisting frame and shear wall structures. In their study the lower bound period of the period interval was set to 20% of the fundamental period and the upper bound period to three times the fundamental period. Also, Kazantzi and Vamvatsikos [18] compared the effectiveness of several IMs based on the geometric mean concept superposing the spectral acceleration read at different logarithmically and linearly equally spaced periods. In this study an IM that combines the spectral acceleration read at five periods ranging from the second-mode period to twice the first-mode period was found to perform best in terms of efficiency and sufficiency across the practical range of peak floor acceleration and interstory drift values of low-rise and high-rise structures.

Adam et al. [19] proposed an optimized IM based on the geometric mean of spectral pseudo-acceleration for evaluating collapse capacity of multi-story moment-resisting frames vulnerable to global P-delta effects. This IM considers for first time a lower bound period of the averaging interval based on the mode in which 95% of the effective modal mass is exceeded. This paper presents the results of a parametric study on the efficiency of the latter IM [19] to prove its superiority over other classical spectral acceleration based IMs when predicting the collapse capacity of P-delta vulnerable structures.

2. Assessed Spectral Acceleration Based Intensity Measure

In this study the efficiency of a spectral acceleration based IM for predicting the collapse capacity of P-delta vulnerable regular frame structures is evaluated. This intensity measure is composed of the geometric mean of n discrete spectral acceleration values $S_a(T^{(i)})$ ($i=1,...,n$) [4]

$$S_{a,gm}(T^{(1)},T^{(n)})=\left(\prod_{i=1}^{n}S_a(T^{(i)})\right)^{1/n} \tag{1}$$

within the period interval ΔT

$$\Delta T=T^{(n)}-T^{(1)},\quad T^{(n)}>T^{(1)} \tag{2}$$

This period interval ΔT has a lower bound period $T^{(1)}$ and an elongated upper bound period $T^{(n)}$. Also, $T^{(i)}$ is the ith period of the set of n periods $T^{(1)},...,T^{(i)},...,T^{(n)}$. In general, $T^{(i)}$ does not comply with a system period T_j. In contrast to Bianchini et al. [4], where S_a is discretized at 10 log-spaced periods within ΔT, in Tsantaki et al. [19] and Kampenhuber [14] S_a is discretized at equally spaced periods $T^{(i)}$ within ΔT (Fig. 1),

$$T^{(i)}=T^{(1)}+\left(i-1\right)\delta T\ ,\quad i=1,...,n\quad ,\quad \delta T=\frac{\Delta T}{n-1}=\frac{T^{(n)}-T^{(1)}}{n-1} \tag{3}$$

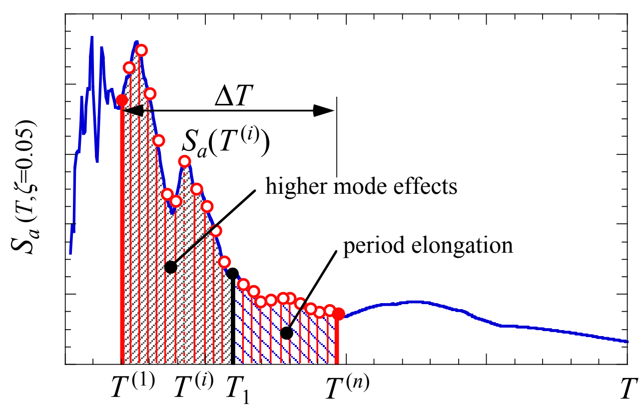

Fig. 1 – Pseudo-acceleration of a ground motion record. Discrete pseudo-accleration values in period interval ΔT. Lower bound period $T^{(1)}$, and upper bound period $T^{(n)}$

In a parametric IDA study on P-delta vulnerable highly inelastic SDOF systems, Tsantaki et al. [15] found that the upper elongated period $T^{(n)}$ leading to the minimum RTR dispersion of the collapse capacity is around $1.6T_{SDOF}$, fluctuating between $1.4T_{SDOF}$ and $2.0T_{SDOF}$. According to this study, for these SDOF systems the "optimal" lower bound period $T^{(1)}$ corresponds to the elastic period, i.e., $T^{(1)}=T_{SDOF}$. The collapse capacity dispersion due to RTR variability of SDOF systems based on the IM $S_{a,gm}(T_{SDOF},1.6T_{SDOF})$ is 50% lower than that obtained from the common IM $S_a(T_{SDOF})$ [15].

In contrast to an SDOF system, for MDOF systems a lower bound interval $T^{(1)}$ of IM $S_{a,gm}(T^{(1)},T^{(n)})$ less than the fundamental period, $T^{(1)}<T_1$, leads to a smaller collapse capacity dispersion, because higher mode effects are accounted for in agreement with Eurocode 8 [20] and ASCE/SEI 41-13 [21] specifications. From a recent study of Adam et al. [19] on various P-Delta vulnerable frame structures exhibiting non-deteriorating and deteriorating characteristics it is concluded that the lower bound period should not be a fixed fraction of the fundamental period T_1 (such as $0.2T_1$ or $0.4T_1$), because such an IM reduces the efficiency for SDOF systems. As a solution it is proposed to relate the lower bound period of averaging interval ΔT, in analogy to Rayleigh damping, with 95% of the total effective cumulative modal mass M, leading to the "optimal" IM [19],

$$IM_{opt} = S_{a,gm}(T_{0.95M}, 1.6T_1) \tag{4}$$

3. Considered Set of Generic Frame Structures Vulnerable to P-Delta

Different sets of generic multi-story frame structures are used to assess the efficiency of the IM defined in Eq. (4) at the collapse limit state. These N story moment-resisting single-bay frame structures of uniform height h, composed of rigid beams and elastic flexible columns, are similar to the ones described in Medina and Krawinkler [22]. To each joint of the frames an identical lumped mass $m_i / 2 = m_s / 2$, i = 1, ... , N, is assigned. According to the weak beam-strong column design philosophy, inelastic rotational springs are located at both ends of the beams and at the base. The bending stiffness of the columns and the initial stiffness of the springs are adjusted to render the desired straight-line fundamental mode shape. The springs exhibit a bilinear backbone curve, whose inelastic branch with reduced stiffness is characterized by the strain hardening coefficient α, which is the same for all springs. The springs strength is tuned to achieve simultaneous initiation of yielding at all spring locations in a static pushover analysis (without gravity loads) under a first mode design load.

A bilinear hysteretic response of the springs is assumed. Unloading stiffness deterioration and cyclic strength deterioration of the bilinear hysteretic cyclic behavior is simulated with the modified Ibarra-Medina-Krawinkler deterioration model [23, 24], but the backbone curve does not consider a negative post-capping stiffness to account for strength deterioration due to large rotational displacements. For the sake of simplicity, the controlling unloading stiffness deterioration and cyclic strength deterioration parameters, Λ_K and Λ_S, respectively, are assumed to be equal for all springs of the frame, $\Lambda_K = \Lambda_S$. Three selected material deterioration levels represent slow, medium, and rapid deterioration [24, 25].

Identical gravity loads are assigned to each story to simulate P-delta effects, implying that axial column forces due to gravity increase linearly from the top to the bottom of each frame. A first mode pushover analysis delivers strong evidence of the vulnerability of a structure to P-delta induced global seismic collapse [26, 30]. If the post-yield stiffness of the global pushover curve becomes negative, during severe seismic excitation, inelastic deformations combined with gravity may cause the structure to approach a state of dynamic instability, and the global collapse limit state is attained at a rapid rate. For the quantification of the P-delta vulnerability a second first mode pushover analysis disregarding gravity loads must be conducted. Then, from the bilinear approximation of both pushover curves the stability coefficients in the elastic range of deformation (θ_e), and the stability coefficient in the post-yield range of deformation (θ_i) can be identified [26, 30]. As an example, the black curve of Fig. 2 illustrates the global pushover curve of a considered frame structure, where the base shear V is plotted against the roof displacement x_N, disregarding the gravity loads in the nonlinear static analysis. The red pushover curve considers gravity loads, leading in this case to a negative post-yield stiffness due to the P-delta effect. Since the considered generic frames are designed for simultaneous yield initiation when subjected to a first mode pushover analysis, both pushover curves are actually bilinear. According to Medina and Krawinkler [22] θ_i can be much larger than θ_e: $\theta_i > (>) \theta_e$. When predicting the collapse capacity of a flexible structure, in many cases cyclic deterioration of the structural components can be disregarded. In those cases, a precondition for seismic collapse is that the post-yield tangent stiffness is negative, or alternatively expressed, the difference of inelastic stability coefficient θ_i and global hardening ratio α_s is larger than zero, i.e., $\theta_i - \alpha_s > 0$, compare with Fig. 2.

Rayleigh damping coefficients were computed by assigning a damping ratio of 5% to the first mode and to the first mode with a cumulative modal mass of at least 95% of the total mass. The corresponding damping matrix is proportional to the mass matrix and the current stiffness matrix.

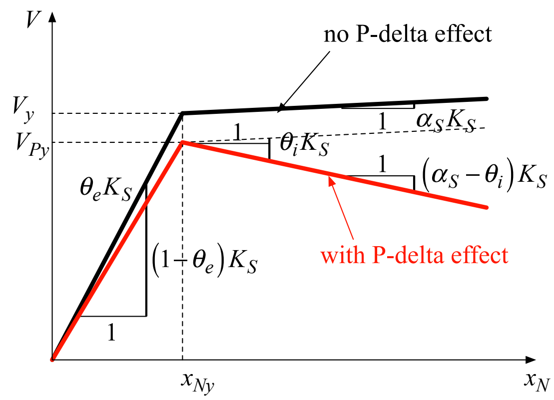

Fig. 2 – Global pushover curve of a considered generic P-delta vulnerable multi-story frame structure (red curve), and the corresponding outcome desregarding gravity loads (black curve) [19]

Collapse capacity dispersion due to RTR variability of the considered P-delta vulnerable multi-story frames is primarily influenced by [8, 19]

- the fundamental period T_1 (without gravity loads),
- the negative slope of the post-yield stiffness $\theta_i - \alpha_S$ in the capacity curve,
- the period elongation due to inelastic deformations, and
- higher modes, correlated with the number of stories N and the structural periods.

In this study the elastic fundamental period T_1, the negative post-yield stiffness ratio $\theta_i - \alpha_S$, and the number of stories N serve as variables. Variation of these parameters affects the fundamental period including the effect of gravity loads, which is subsequently denoted as $T_1^{P\Delta}$. The period elongation at collapse is largely controlled through $\theta_i - \alpha_S$, and deterioration of the unloading stiffness and strength. Thus, results are presented both for frames with non-deteriorating springs and springs subjected to medium deterioration.

In total 2048 generic frame structures are studied. All predefined basic model parameters of the considered generic frame structures are summarized in Table 1.

Table 1 – Range of basic model parameters of the considered generic frame structures

Parameter	Description	Parameter range
N	Number of stories	1, 3, 6, 9, 12, 15, 18, 20
T_1	Fundamental period	0.5, 1.0, 1.5, 2.0, 2.5, 3.0, 3.5, 4.0
$\theta_i - \alpha_S$	Negative post-yield stiffness ratio	0.03, 0.04, 0.05, 0.06, 0.10, 0.20, 0.30, 0.40
α	Strain hardening coefficient of rotational springs	0.03
$\Lambda_K = \Lambda_S$	Deterioration parameter for no deterioration; and slow, medium, and rapid deterioration	∞, 2.0, 1.0, 0.5

4. Collapse Capacity and its Record-to-Record Variability

The Incremental Dynamic Analysis (IDA) procedure is used to predict the collapse capacity. An IDA consists of a series of time history analysis, in which the intensity of a particular ground motion is monotonically increased. As a result, the IM is plotted against the EDP (here the roof drift). The procedure is stopped when this parameter grows unbounded, indicating structural collapse. The corresponding IM, $IM_i|_{collapse}$, is referred to as the structural collapse capacity subjected to that particular ground motion record indicated by subscript i,

$$CC_i = IM_i\big|_{collapse} \tag{5}$$

Since the collapse capacity is highly record dependent, this quantity is computed for each record of the selected ground motion set, and subsequently evaluated statistically. According to Shome and Cornell [28] the set of corresponding collapse capacities can be represented by a log-normal distribution. The log-normal distribution is characterized by the median $\mu_{\ln CC}$ of the natural logarithm and the standard deviation β of the logarithm of individual collapse capacities [29],

$$\beta = \sqrt{\sum_{i=1}^{r} \frac{(\ln CC_i - \mu_{\ln CC})^2}{r-1}} \tag{6}$$

r is the number of utilized ground motion records, and thus, of the individual collapse capacities, CC_i, $i = 1,...,r$.

Ground motion induced uncertainties of the collapse capacity of the testbed structures are computed employing the far-field ground motions of the LMSR-N record set [22]. The LMSR-N bin contains 40 ground motions recorded in California on NEHRP site class D during earthquakes of moment magnitude M_w between 6.5 and 7 and closest distance to the fault rupture between 13 km and 40 km. This set of records has strong motion duration characteristics insensitive to magnitude and distance [22].

5. Efficiency Study

Subsequently, the efficiency of the "optimal" intensity measure IM_{opt} is qualitatively and quantitatively assessed. Fig. 3 shows dispersion parameter β for nine sets of frames with non-deteriorating material properties subjected to the 40 LMSR-N ground motions based on IM_{opt}, and for comparison also for four additional IMs. The "classical" IM $S_a(T_1)$, i.e. the spectral pseud-acceleration read at the fundamental period (without gravity) T_1, serves as benchmark. The spectral pseudo-acceleration at the fundamental period affected by P-delta, $S_a(T_1^{P\Delta})$, is the second comparative IM. The geometric mean IM $S_{a,gm}(T_1,1.6T_1)$ with lower bound T_1 and upper bound $1.6T_1$ considers the effect of period elongation, while IM $S_{a,gm}(0.2T_1,1.6T_1)$ also covers the higher modes. In contrast to IM_{opt} in IM $S_{a,gm}(0.2T_1,1.6T_1)$ the lower bound is a fixed value, i.e. $0.2T_1$. As observed, for all structures IM_{opt} is more efficient than both single target IMs $S_a(T_1)$ and $S_a(T_1^{P\Delta})$. Moreover, for the majority of structures it is the most efficient IM, and in the remaining cases, the deviation to the most efficient one is no more than 5%. The plots in Fig. 3 group the frames according to the number of stories N (Figs 3a-c), the negative post-yielding stiffness ratio (Figs 3d-f), and the period of vibration (Figs 3g-i).

In Figs 3a, 3b, and 3c the collapse capacity variability is presented as a function of the number of stories N, for frames that have the same period $T_1 = 3.5s$, but different $\theta_i - \alpha_S$. As observed, the collapse capacity dispersion increases as the number of stories increases. For the two frame sets with significant P-delta effect (i.e., $\theta_i - \alpha_S$ is 0.10 and 0.20) the dispersion reduction based on IM_{opt} is between 20 and 40% compared to IM $S_a(T_1)$, see Figs 3b and c. In contrast, the efficiency increase of IM_{opt} for structures exposed to moderate P-delta effect ($\theta_i - \alpha_S = 0.03$) is 5 to 14% only (Fig. 3a). These figures also show that for one-story structures IM_{opt} with variable lower bound period is more efficient than IM $S_{a,gm}(0.2T_1,1.6T_1)$ with fixed lower bound period, in particular if $\theta_i - \alpha_S$ becomes large. In those cases, however, IM $S_{a,gm}(T_1,1.6T_1)$ exhibits the same efficiency than IM_{opt}, because obviously an SDOF system has no higher modes to be considered in the IM definition. Thus, it can be concluded that IM_{opt} combines the advantages of IMs $S_{a,gm}(T_1,1.6T_1)$ and $S_{a,gm}(0.2T_1,1.6T_1)$ without the necessity to distinguish between one-story and multi-story structures when selecting the appropriate IM. For the long-period structures, $T_1 = 3.5s$, with various parameter configurations shown in this figure both single-target IMs $S_a(T_1)$ and $S_a(T_1^{P\Delta})$ lead to a similar efficiency of the collapse capacity prediction with the exception of the one-story frame with $\theta_i - \alpha_S = 0.20$ where $S_a(T_1^{P\Delta})$ is significantly more efficient, see Fig. 3c.

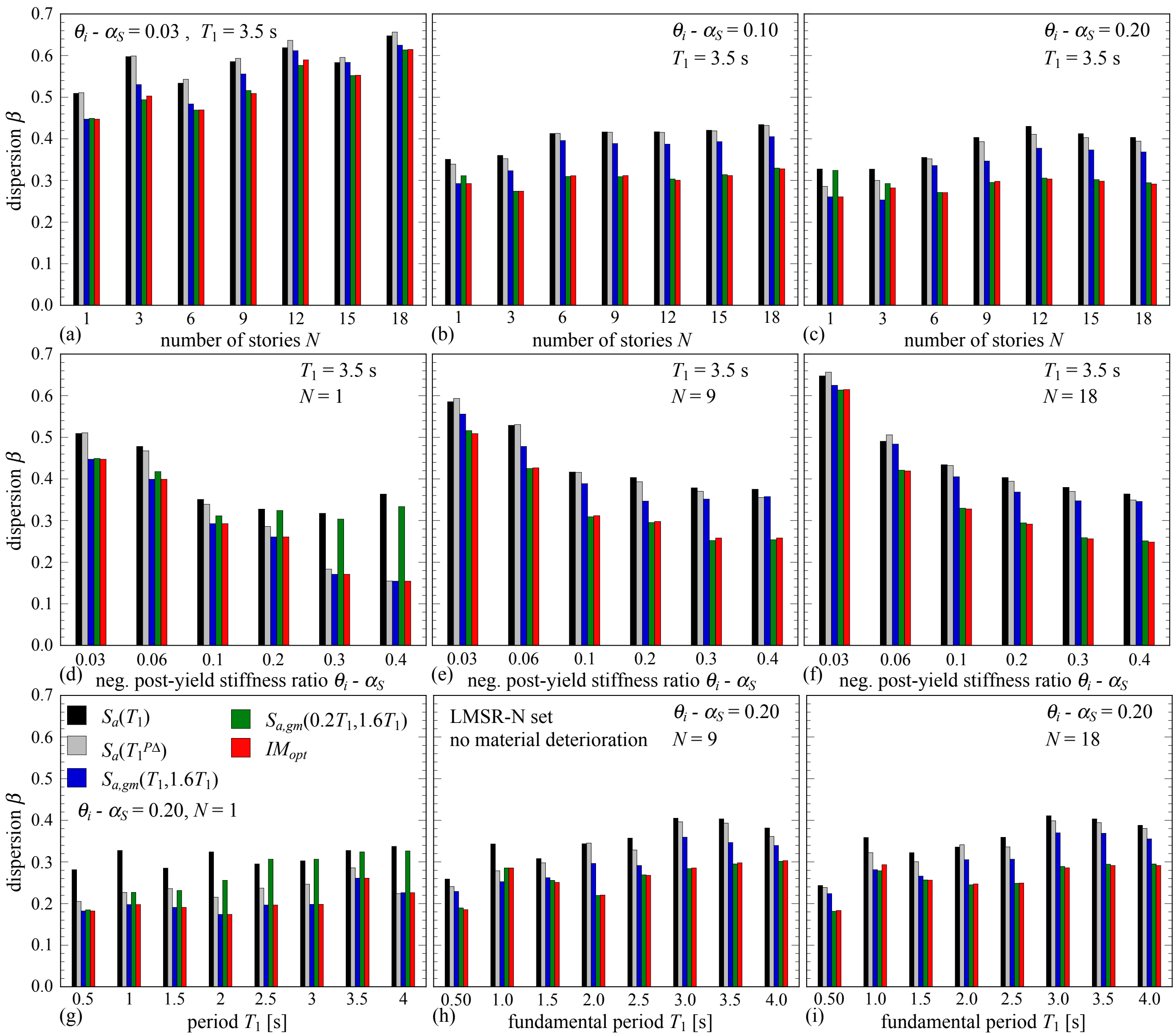

Fig. 3 – Dispersion of the collapse capacity for nine frame sets with parameters as specified. No material deterioration. Benchmark IM $S_a(T_1)$, IM $S_a(T_1^{P\Delta})$, one IM considering period elongation, one IM considering both period elongation and higher mode effects as specified, and "optimal" IM IM_{opt}. LMSR-N record set

Figs 3d, 3e, and 3f show the collapse variability for flexible frames with a fundamental period of 3.5s as a function of the negative post-yield stiffness ratio for frames of one (Fig. 3d), nine (Fig. 3e), and 18 (Fig. 3f) stories. These figures confirm that collapse capacity dispersion decreases for systems with a steeper $\theta_i - \alpha_S$, because they are more prone to collapse and less dependent on RTR variability. For instance, for IM_{opt} the nine-story structure with $\theta_i - \alpha_S = 0.03$ exhibits dispersion $\beta = 0.51$, for $\theta_i - \alpha_S = 0.40$ it decreases to $\beta = 0.26$. Also, IM_{opt} is more efficient on SDOF frames with a large negative post-yield stiffness ratio. For instance, for the one-story frame with $\theta_i - \alpha_S = 0.40$ the IM_{opt} dispersion is only 42% of the dispersion based on IM $S_a(T_1)$. For this structural configuration the dispersion based on the single-target IM $S_a(T_1^{P\Delta})$ is of the same order as for IM $S_a(T_1)$. On average the reduction of the dispersion based on IM_{opt} is about 20% compared to benchmark IM $S_a(T_1)$. The results for the one-story frames confirm that with increasing $\theta_i - \alpha_S$ the efficiency of IM_{opt} becomes larger compared to $S_{a,gm}(0.2T_1, 1.6T_1)$. For the same structures the collapse dispersion for IM $S_a(T_1^{P\Delta})$ is in the same order as for IM_{opt}, and thus, much smaller than for IM $S_a(T_1)$.

The effect of different fundamental periods of vibration in 1-, 9-, and 18-story frames is presented in Figs 3g, 3h, and 3i, respectively. The parameter $\theta_i - \alpha_S = 0.20$ is constant, and periods T_1 between 0.5 and 4.0s are spaced at 0.5s in the three frame sets. Figs 3g to 3i show that the dispersion is not significantly affected by period T_1. More important for dispersion is the number of stories. While for one-story structures and IM_{opt} the variability β fluctuates around 0.20, for the nine-story and 18-story frames it is in average 0.26. The efficiency enhancement of IM_{opt} compared to that of IM $S_a(T_1)$ does not follow a uniform trend. However, it is more pronounced for SDOF systems than for the multi-story frames, as discussed before. The results confirm that both for one-story and multistory frames IM_{opt} is in general most efficient. For SDOF systems the efficiency of IM_{opt} and IM $S_{a,gm}(T_1, 1.6T_1)$ is identical, and for IM $S_a(T_1^{P\Delta})$ closer to IM_{opt} than to IM $S_a(T_1)$. For MDOF systems the efficiency of IM_{opt} and IM $S_{a,gm}(0.2T_1, 1.6T_1)$ is similar.

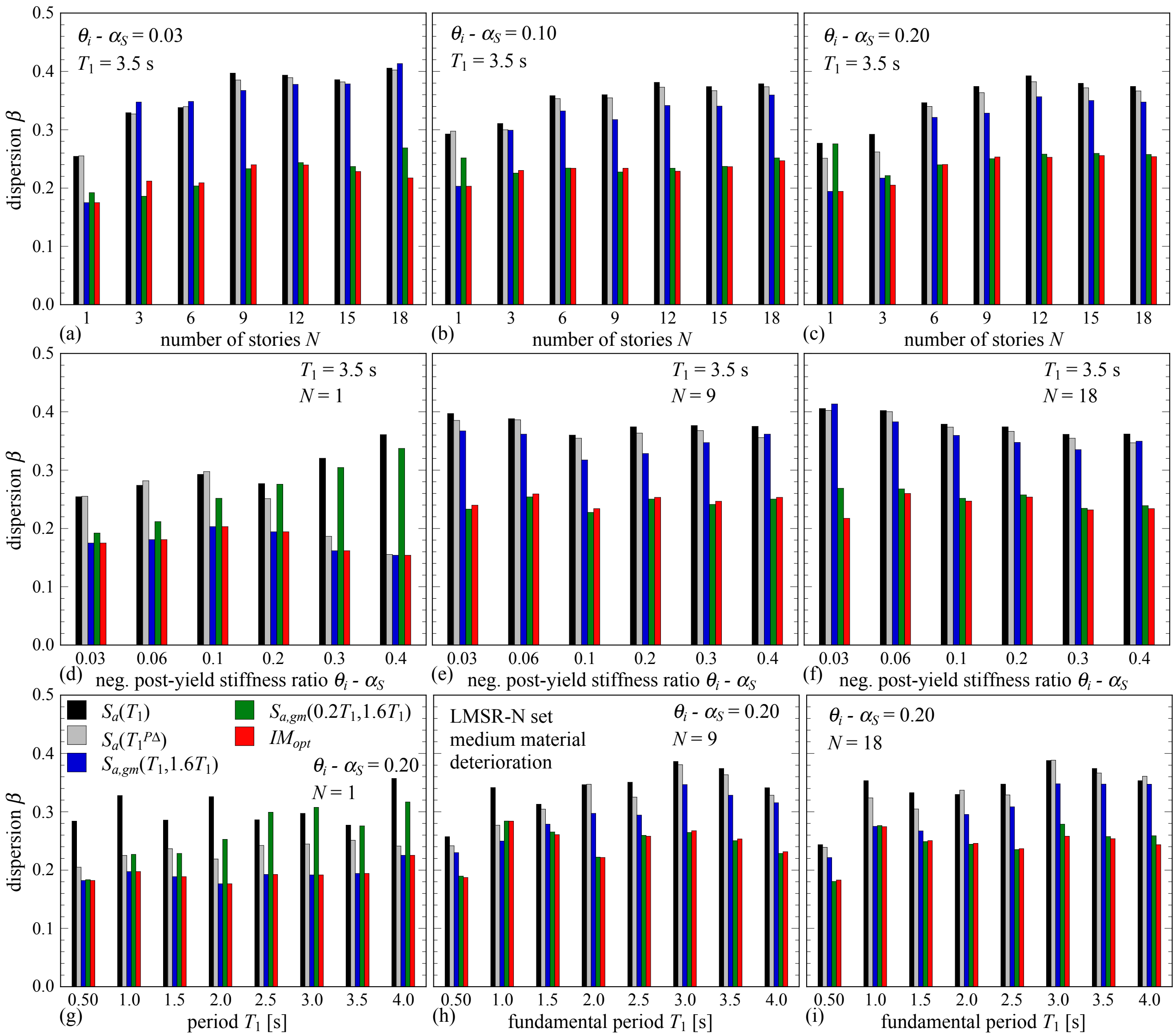

Fig. 4 Dispersion of the collapse capacity for nine frame sets with parameters as specified. Medium material deterioration. Benchmark IM $S_a(T_1)$, IM $S_a(T_1^{P\Delta})$, one IM considering period elongation, one IM considering both period elongation and higher mode effects as specified, and "optimal" IM IM_{opt}. LMSR-N record set

Subsequently, it is investigated whether the findings for material non-deteriorating P-delta vulnerable frames can be transferred to structures that also are exposed to material deterioration, as defined in Table 1. Fig. 4 shows the collapse capacity dispersion for similar generic frames to those of Fig. 3, but with medium deterioration of strength and stiffness. To quantify the efficiency enhancement of the alternative IMs with respect to the benchmark IM $S_a(T_1)$, Fig. 5 represents the ratio of the dispersion of the four alternative IMs with respect to β based on IM $S_a(T_1)$.

Comparison of the outcomes of Figs 3. and 4 reveals that the general trend of β with respect to the number of stories N, negative post-yield stiffness ratio $\theta_i - \alpha_S$, and fundamental period T_1 is the same, confirming the superior IM_{opt} efficiency. However, the magnitude of β becomes (much) smaller compared to the non-deteriorating counterparts; in particular, if the negative post-yield stiffness ratio is small, i.e. $\theta_i - \alpha_S = 0.03$. For instance, for the first frame set, whose results are shown in Figs 3a and 4a, consideration of medium material deterioration reduces the dispersion β to 50% compared to the non-deteriorating systems.

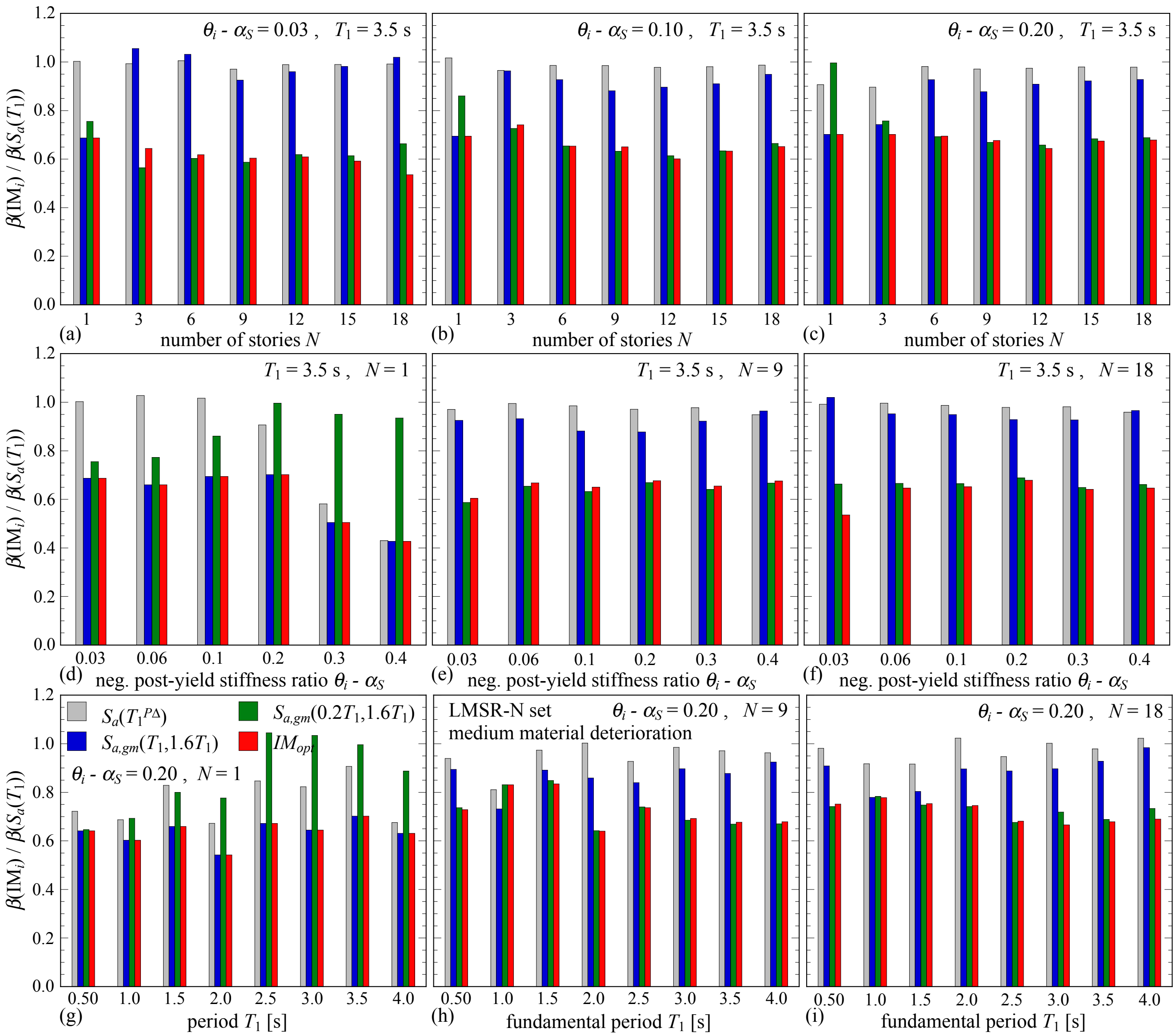

Fig. 5 Dispersion of the collapse capacity based on alternative IMs over the dispersion for benchmark IM $S_a(T_1)$. Nine frame sets with parameters as specified. Medium material deterioration. LMSR-N record set

Note that the efficiency of IM_{opt} with respect to the benchmark IM $S_a(T_1)$ significantly improves. The corresponding plots of the collapse capacity ratios of Fig. 5 show that the efficiency enhancement is on average about 30%, compared to 20% for non-deteriorating frames.

The three-dimensional bar plots of Figs 6 and 7 provide a global overview of collapse capacity dispersion. Fig. 6 shows the dispersion based on IMs $S_a(T_1)$ and IM_{opt} for a set of medium deteriorating frames with $\theta_i - \alpha_S = 0.20$ as a function of period T_1 and number of stories N. Additionally, the dispersion ratio for these two IMs is depicted. The structures of Fig. 7 have a period of $T_1 = 3.5s$, and the dispersion is plotted against $\theta_i - \alpha_S$ and N.

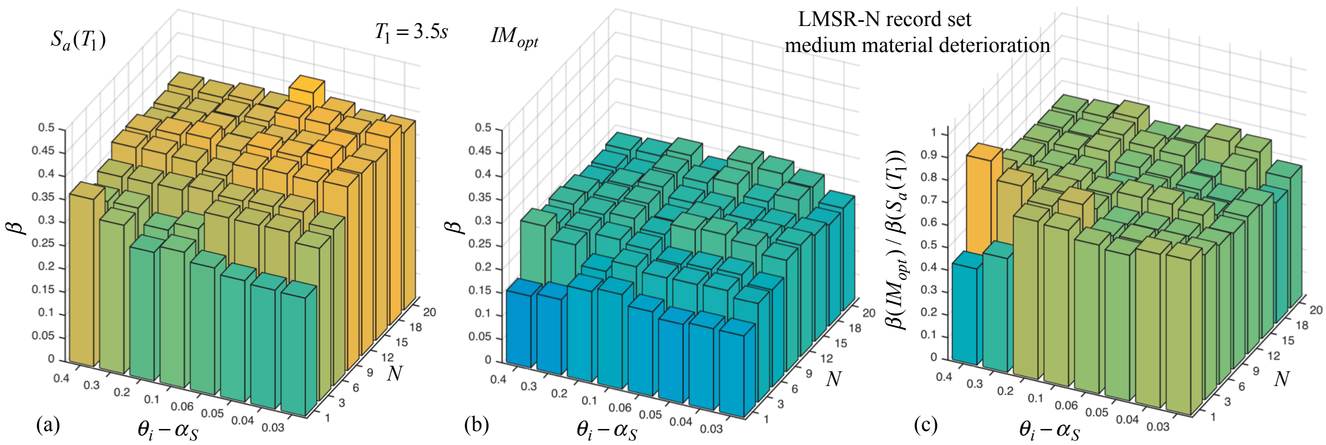

Fig. 6 Dispersion of the collapse capacity for 72 frames with $\theta_i - \alpha_S = 0.20$ plotted against the number of stories and the fundamental period. (a) IM $S_a(T_1)$, (b) IM IM_{opt}, (c) dispersion ratio. Medium material deterioration. LMSR-N record set

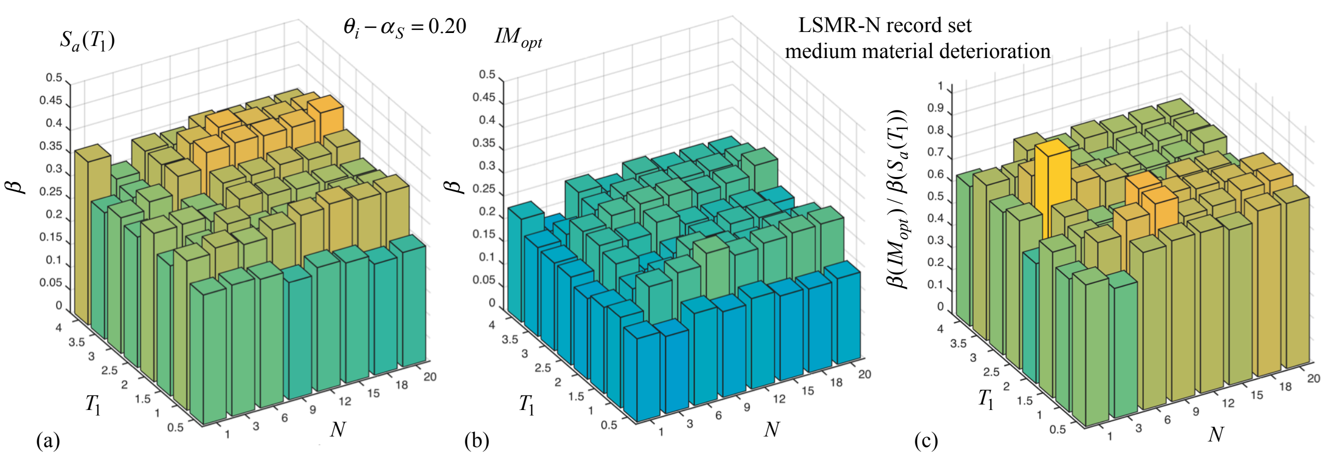

Fig. 7 Dispersion of the collapse capacity for 64 frames with $T_1 = 3.50s$ plotted against the number of stories and the negative post-yield stiffness ratio. (a) IM $S_a(T_1)$, (b) IM IM_{opt}, (c) dispersion ratio. Medium material deterioration. LMSR-N record set

6. Summary and Conclusions

In this study an "optimized" spectral acceleration based intensity measures (IMs) for P-delta vulnerable generic moment-resisting frames at their collapse limit state has been assessed. This "optimal" IM, IM_{opt}, is based on the geometric mean of the spectral pseudo-acceleration, $S_{a,gm}$, over a certain period interval. The "optimal" upper bound of the period interval for the geometric mean IM is 1.6 times the system period without consideration of gravity loads. Thus, period elongation either a result of large inelastic deformations in the case of small negative post-yield stiffness slopes, or the result of the presence of gravity loads in systems with steeper slopes is covered. The IM optimization is achieved by using a lower bound corresponding to the structural period associated with the exceedance of 95% of the total effective mass. In a parametric study considering a set of 2048 generic frames the efficiency of these IM to reduce collapse capacity dispersion due to the record-to-record (RTR) variability has been evaluated, and compared to two single target spectral IMs and to two geometric mean of the spectral pseudo-acceleration based IMs. The single target spectral IMs are the 5% damped spectral pseudo-accelerations $S_a(T_1)$ and $S_a(T_1^{P\Delta})$ at the elastic fundamental period without and with consideration of gravity loads, T_1 and $T_1^{P\Delta}$, respectively. The intensity measure IM $S_{a,gm}(T_1,1.6T_1)$, with the lower bound period T_1 and the upper bound period $1.6T_1$, considers the effect of period elongation only; while $S_{a,gm}(0.2T_1,1.6T_1)$, with the fixed lower bound period $0.2T_1$, also covers higher mode effects. The collapse capacity dispersion due to record-to-record variability of the evaluated structures is mainly affected by the fundamental period T_1, the negative post-yield stiffness ratio $\theta_i - \alpha_S$, the number of stories *N*, and material deterioration. From the results of this parametric study it can be concluded that IM_{opt} is in general more efficient than the considered benchmark IMs. This IM allows a consistent "optimal" representation for both SDOF and MDOF systems. In particular the enhancement with respect to the traditional benchmark IM $S_a(T_1)$ the efficiency of efficiency of IM_{opt} increases in average up to 30%. The results and conclusions of this study are valid only for P-delta vulnerable hysteretic systems, where the post-capping range of deformation is not attained.

7. Acknowledgements

This work was partially supported by the Austrian Ministry of Science BMWF as part of the "UniInfrastrukturprogramm" of the Focal Point Scientific Computing at the University of Innsbruck.

8. References

[1] Cordova PP, Deierlein GG, Mehanny SSF, Cornell CA (2001): Development of two-parameter seismic intensity measure and probabilistic assessment procedure. *Proc. Second U.S.-Japan Workshop on Performance-based Earthquake Engineering Methodology for Reinforced Concrete Buildings Structures*, Sapporo, Japan, pp. 187-206.

[2] Haselton CB, Baker JW (2006): Ground motion intensity measures for collapse capacity prediction: choice of optimal spectral period and effect of spectral shape. *Proc. 8th National Conference on Earthquake Engineering*, San Francisco, CA, 18-22 April 2006, 10 pp.

[3] Luco N, Cornell CA (2007): Structure-specific scalar intensity measure for near-source and ordinary earthquake motions. *Earthquake Spectra*, **23**, 357-391.

[4] Bianchini M, Diotallevi P, Baker JW (2009): Prediction of inelastic structural response using an average of spectral accelerations. *Proc. 10th International Conference on Structural Safety and Reliability (ICOSSAR 09)*, Osaka, Japan, 13-19 September 2009, 8 pp.

[5] Kadas K, Yakut A, Kazaz I (2011): Spectral ground motion intensity based on capacity and period elongation. *Journal of Structural Engineering*, **137**, 401-409.

[6] Vamvatsikos D, Cornell CA (2005): Developing efficient scalar and vector intensity measures for IDA capacity estimation by incorporating elastic spectral shape information. *Earthquake Engineering & Structural Dynamics*, **34**, 1573-1600.

[7] Bojórquez E, Iervolino I (2011): Spectral shape proxies and nonlinear structural response. *Soil Dynamics and Earthquake Engineering*, **31** (7), 996-1008.

[8] Adam C, Tsantaki S, Ibarra LF, Kampenhuber D (2014): Record-to-record variability of the collapse capacity of multi-story frame structures vulnerable to P-delta. *Proc. Second European Conference on Earthquake Engineering and Seismology (2ECEES)*, Istanbul, Turkey, August 24-29 2014, electronic volume (ISBN: 978-605-62703-6-9), 12 pp.

[9] Eads L, Miranda E, Lignos DG (2015): Average spectral acceleration as an intensity measure for collapse risk assessment. *Earthquake Engineering & Structural Dynamics*, **44** (12), 2057-2073.

[10] Baker JW. Cornell CA (2005): A vector-valued ground motion intensity measure consisting of spectral acceleration and epsilon. *Earthquake Engineering & Structural Dynamics*, **34**, 1193-1217.

[11] Jalayer F, Beck JL, Zareian F (2012): Information-based relative sufficiency of some ground motion intensity measures. *Proc. 15th World Conference on Earthquake Engineering (15 WCEE)*, Lisbon, Portugal, September 24-28, digital paper, paper no 5176, 10 pp.

[12] O'Donnell AP, Kurama YC, Kalkan E, Taflanidis AA, Beltsar OA (2013): Ground motion scaling methods for linear-elastic structures: An integrated experimental and analytical investigation. *Earthquake Engineering & Structural Dynamics*, **42**, 1281-1300.

[13] Tsantaki S (2014): *A contribution to the assessment of the seismic collapse capacity of basic structures vulnerable to the destabilizing effect of gravity loads*. Doctoral thesis, University of Innsbruck.

[14] Kampenhuber D (2016): *Simplified collapse fragility assessment utilizing a geometric mean spectral acceleration based intensity measure for PDelta vulnerable, cyclic deteriorating frame structures*. Doctoral thesis, University of Innsbruck.

[15] Tsantaki S, Adam C, Ibarra LF (2016): Intensity measures that reduce collapse capacity dispersion of P-delta vulnerable simple systems. *Bulletin of Earthquake Engineering*, online (DOI: 10.1007/s10518-016-9994-4).

[16] Adam C, Jäger C (2012): Seismic collapse capacity of basic inelastic structures vulnerable to the P-delta effect. *Earthquake Engineering & Structural Dynamics*, **41**, 775-793.

[17] Jäger C, Adam C (2013): Influence coefficients for collapse capacity spectra. *Journal of Earthquake Engineering*, **17**, 859-878.

[18] Kazantzi A, Vamvatsikos D (2015): Intensity measure selection for vulnerability studies of building classes. *Earthquake Engineering & Structural Dynamics*, **44**, 2677-2694.

[19] Adam C, Kampenhuber D, Ibarra LF, Tsantaki S (2016): Optimal spectral acceleration based intensity measure for seismic collapse assessment of P-delta vulnerable frame structures. *Journal of Earthquake Engineering*, online (DOI: 10.1080/13632469.2016.1210059).

[20] Eurocode 8 (2004): Design provisions of structures for earthquake resistance. Part 1: General rules, seismic actions and rules for buildings.

[21] ASCE/SEI 41-13 (2014) Seismic Evaluation and Retrofit of Existing Buildings. American Society of Civil Engineers, Reston, Virginia, U.S.A.

[22] Medina RA, Krawinkler H (2003): Seismic demands for nondeteriorating frame structures and their dependence on ground motions. *Report No. 144*. The John A. Blume Earthquake Engineering Research Center, Department of Civil and Environmental Engineering, Stanford University, Stanford, CA.

[23] Ibarra L, Krawinkler H (2011): Variance of collapse capacity of SDOF systems under earthquake excitations. *Earthquake Engineering & Structural Dynamics*, **40**, 1299-1314.

[24] Lignos DG, Krawinkler H (2012): Sidesway collapse of deteriorating structural systems under seismic excitations. *Report No. 177*. The John A. Blume Earthquake Engineering Research Center, Department of Civil and Environmental Engineering, Stanford University, Stanford, CA.

[25] Lignos DG, Krawinkler H (2011): Deterioration modeling of steel components in support of collapse prediction of steel moment frames under earthquake loading. *Journal of Structural Engineering*, **137** (11), 1291-1302.

[26] Adam C, Jäger C (2012): Simplified collapse capacity assessment of earthquake excited regular frame structures vulnerable to P-delta. *Engineering Structures*, **44**, 159-173.

[27] Adam C, Ibarra LF (2015): Seismic collapse assessment. *Earthquake Engineering Encyclopedia*, **Vol. 3** (Beer M, Kougioumtzoglou IA, Patelli E, Siu-Kui Au I, eds), 2729-2752, Springer Berlin Heidelberg.

[28] Shome N, Cornell CA (1999): Probabilistic seismic demand analysis of nonlinear structures. *RMS Tech Report No. 38*. The John A. Blume Earthquake Engineering Research Center, Department of Civil and Environmental Engineering, Stanford University, Stanford, CA.

[29] FEMA-350 (2000): Recommended seismic design criteria for new steel moment-frame buildings. *Report No. FEMA-350*, SAC Joint Venture, Federal Emergency Management Agency, Washington DC, USA.

[30] Ibarra LF, Krawinkler H (2005): Global collapse of frame structures under seismic excitations. *Report No. 152*. The John A. Blume Earthquake Engineering Research Center, Department of Civil and Environmental Engineering, Stanford University, Stanford, CA.